December 9, 1999
ANAG/URE/SPQ3

Final Technical Report

SOLPOL – A Solar Polarimeter for Hard X-Rays and Gamma-Rays

NASA Grant NAG5-7294
Period of Performance: April 15, 1998 to October 15, 1999
(includes 6-month no-cost extension)

Principal Investigator :
Dr. Mark L. McConnell
University of New Hampshire

Summary

Th goal of this project was to continue the development of a hard X-ray polarimeter for studying solar flares. In earlier work (funded by a previous SR&T grant), we had already achieved several goals, including the following: 1) development of a means of producing a polarized radiation source in the lab that could be used for prototype development; 2) demonstrated the basic Compton scatter polarimeter concept using a simple laboratory setup; 3) used the laboratory results to verify our Monte Carlo simulations; and 4) investigated various detector technologies that could be incorporated into the polarimeter design. For the current one-year program, we wanted to fabricate and test a laboratory science model based on our SOLPOL design. The long-term goal of this effort is to develop and test a prototype design that could be used to study flare emissions from either a balloon- or space-borne platform.

The current program has achieved its goal of fabricating and testing a science model of the SOLPOL design, although additional testing of the design (and detailed comparison with Monte Carlo simulations) is still desired. This one-year program was extended by six months (no-cost extension) to cover the summer of 1999, when undergraduate student support was available to complete some of the laboratory testing.

Earlier Work

In order to effectively work in the laboratory to develop a hard X-ray polarimeter, it is necessary to provide a ready source of polarized hard X-ray photons. We have achieved this goal by scattering photons from a radioactive source off a block of plastic scintillator. Not only does the scattering itself result in a polarization of the scattered beam, the use of a plastic scintillator provides a means of electronically tagging the polarized photon beam.

The basic concept for polarization at hard X-ray energies uses Compton scattering. Our laboratory demonstration was based on a semi-circular array of plastic scintillators centered on a single NaI scintillator. This arrangement not only demonstrated the basic principle of a Compton scatter polarimeter, but it served to verify the integrity of our

polarized photon source and our Monte Carlo simulations. In all regards, these laboratory tests were quite successful.

Results from the laboratory setup were used to verify our GEANT-based Monte Carlo software. We collected data using a polarized beam at various polarization angles. Not only was the shift in polarization angle verified, but the modulation factors predicted by the Monte Carlo data were also verified. These results gave us confidence in the reliability of our Monte Carlo software.

SOLPOL - A Prototype Design

Our work on polarimeter development has led to a modular design concept that employs an array of plastic scintillators mounted on the front end of a 5" diameter position-sensitive photomultiplier tube (PSPMT). We refer to this design as SOLPOL - a SOLar POLarimeter for hard X-rays and gamma-rays (Figure 1). Initially, we had considered the use of a scintillating fiber bundle, but recent laboratory tests have clearly demonstrated that, for the geometries we are considering (5mm square by 3" long), that the light output of an array of individual scintillator segments is far superior to that of a scintillating fiber bundle. Light output is an important factor in our design in that it determines the lower energy threshold of the polarimeter device. A higher light output is required to achieve a lower threshold. Monte Carlo simulations of this design (see attached references) indicate that an array of these modules could be used to effectively study solar flare hard X-ray polarizations in the 50-300 keV energy band.

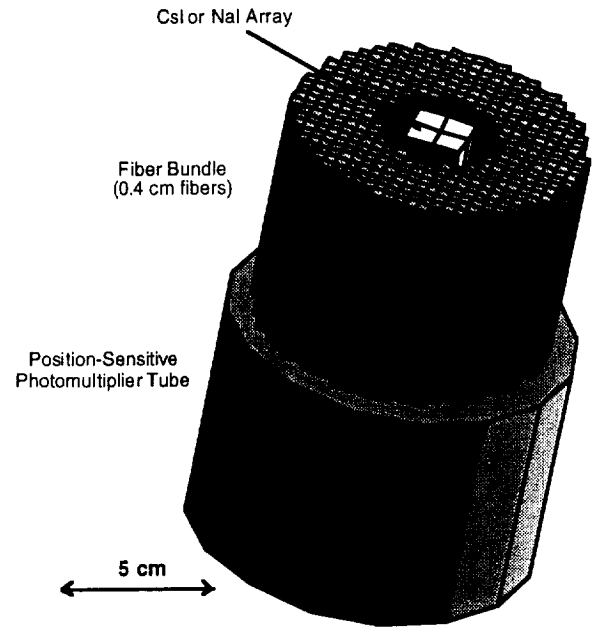

Figure 1: A schematic of the SOLPOL polarimeter design.

SOLPOL Science Model Fabrication

During the current funding period, we acquired the various components of the SOLPOL science model and fabricated the complete assembly. The various components of the assembly are shown in Figure 2, including the MAPMT / CsI array, the plastic scintillator array and the 5-inch PSPMT. The completed assembly is fit into a light-tight aluminum housing. Hard X-ray photons incident on the fron surface of the device first interact in the plastic scintillator array (viewed by a 5-inch PSPMT) and then scatter into a central CsI array (viewed by a 2x2 MAPMT). The scatter angle of each event (as it scatters from the plastic into the CsI) is then reconstructed based on the event data. The distribution of these scatter angles is used to search for and identify the polarization signal in the data. In principle, the data can be used to determine not only the level of linear polarization, but also the angle of the polarization. Data acquisition from the assembled unit was achieved using CAMAC modules coupled via a SCSI interface to a Macintosh computer.

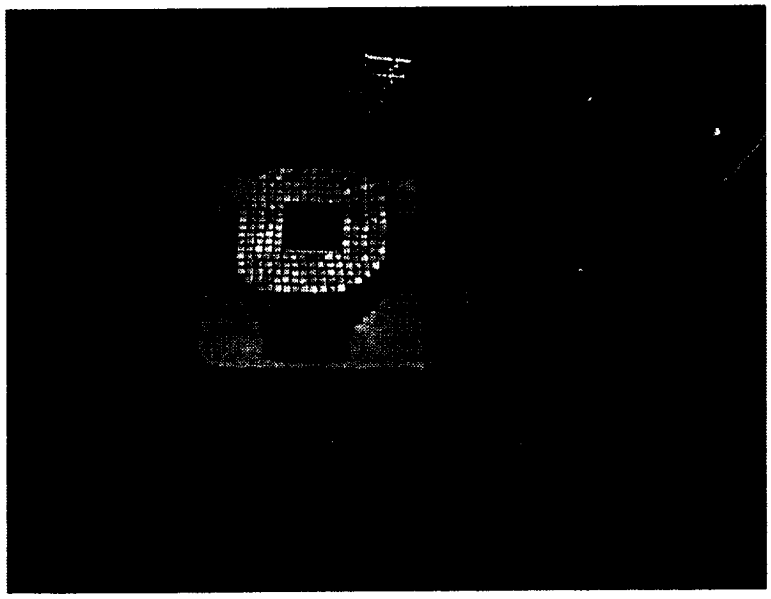

Figure 2: Components of the SOLPOL science model.

SOLPOL Science Model Testing

The initial laboratory tests were designed to demonstrate the ability to locate events within the plastic array using the outputs of the PSPMT. (In this case, we are using only the charge-division readouts of the PSPMT for event localization, rather than the full suite of 56 anode signal wires that, in principle, are available for readout.) Figure 3 shows that the events are sufficiently well-localized to resolve the individual (5 mm) plastic elements within the array. This suggests that a finer level of spatial localization might be achievable with smaller plastic elements.

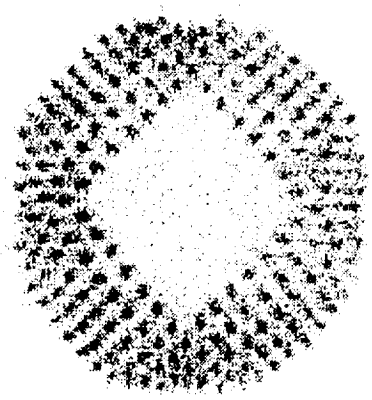

Figure 3: Measured distribution of events within the plastic array.

Testing with the complete assembly and a polarized photon source allowed us to search for a polarization signal in the data. For various reasons (e.g., hardware failures, low source flux), we have only limited polarimetric data from the completed assembly. The low level of statiustics available in these first runs preclude a detailed quantitative analysis. The initial results, shown in Figure 4, demonstrate the presence of a polarization signal. These results, although not very quantitative at the moment, demonstrate that the SOLPOL design is a viable one for measuring hard X-ray polarization.

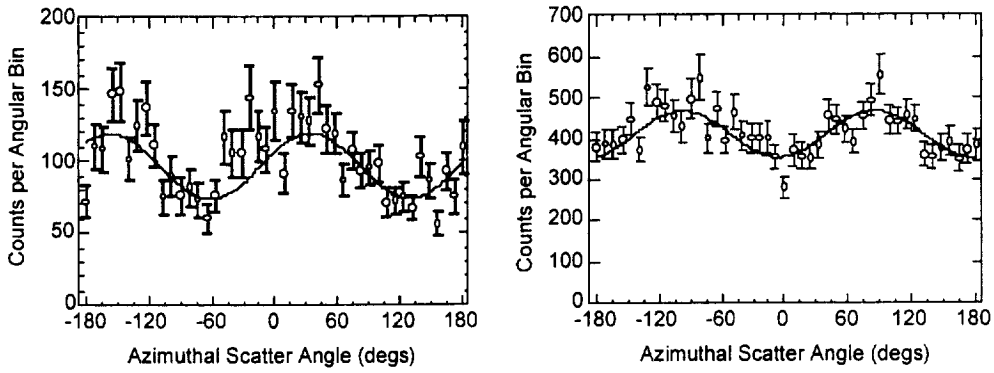

Figure 4: Demonstration of a polarization signal from the SOLPOL science model, as shown by the polarimetric response at two different polarization angles offset by ~45° with photons of ~360 keV..

Future Work

Pending the receipt of additional funding for our development efforts, we would pursue the continued testing with the SOLPOL science model. These efforts would concentrate on improved data from the science model that would facilitate a more quantitative assessment of the SOLPOL science model performance. We would also draw upon our experience to date to improve the hardware. In particular, this would include better fabrication approach for the MAPMT / CsI assembly and an alternative readout scheme for the PSPMT that would provide more detailed spatial information with improved rejection capability for multiple scatter events. Additional work would concentrate on the packaging and also on alternative, but related, designs that might be more amenable to spaceflight applications. A

low level of development of this concept would allow us to provide useful instrumentation during the slar maximum of 2012.

Publications

Recent presentations and publications include the following (copies of items 1, 3 and 4 are attached to this report):

1) *Development of a Hard X-Ray Polarimeter forAstrophysics*
M.L. McConnell, J. Macri, M. McClish, J. Ryan, D.J. Forrest, and W.T. Vestrand, 1999, IEEE Trans. Nucl. Sci., 46, No. 4, 890.

2) *Laboratory Testing of a Hard X-Ray Solar Polarimeter*
M.L. McConnell, J. Macri, M. McClish, and J.M. Ryan, paper presented at the 194th Meeting of the American Astronomical Society (Solar Physics Division), Chicago, IL (June, 1999).

3) *Recent Laboratory Tests of A Hard X-Ray Solar Flare Polarimeter*
M.L. McConnell, J. Macri, M. McClish, and J.M. Ryan, paper presented at the International Symposium on Optical science, Engineering and Instrumentation (SPIE), Denver, CO (July, 1999), to be published in Proc. SPIE (1999).

4) *A Polarimeter for Studying Hard X-Rays from Solar Flares*
M.L. McConnell, J. Macri, M. McClish, and J.M. Ryan, 1999, in proceedings of the 26th International Cosmic Ray Conference, Salt Lake City, UT (August, 1999), Vol. 6, p. 21.

5) *A Modular Hard X-Ray Polarimeter for Solar Flares*
M.L. McConnell, J. Macri, M. McClish, and J.M. Ryan, paper presented at the High Energy Solar Physics Workshop (Anticipating HESSI), College Park, MD (October, 1999), to be published in AIP Conf. Proc.

IEEE Trans. Nucl. Sci., Vol. 46(4), 890. (1999)

Development of a Hard X-Ray Polarimeter for Astrophysics

M.L. McConnell, J.R. Macri, M. McClish, J. Ryan, D.J. Forrest and W.T. Vestrand
Space Science Center, Morse Hall, University of New Hampshire, Durham, New Hampshire 03824

Abstract

We have been developing a Compton scatter polarimeter for measuring the linear polarization of hard X-rays (100-300 keV) from astrophysical sources. A laboratory prototype polarimeter has been used to successfully demonstrate the reliability of our Monte Carlo simulation code and to demonstrate our ability to generate a polarized photon source in the lab. Our design concept places a self-contained polarimeter module on the front-end of a a 5-inch position-sensitive PMT (PSPMT). We are currently working on the fabrication of a science model based on this PSPMT concept. Although the emphasis of our development effort is towards measuring hard X-rays from solar flares, our design has the advantage that it is sensitive over a rather large field-of-view (> 1 steradian), a feature that makes it especially attractive for γ–ray burst studies.

I. INTRODUCTION

The basic physical process used to measure linear polarization of hard X-rays (100–300 keV) is Compton scattering [1]. The scattering geometry can be described by two angles. The first of these is the Compton scatter angle (θ),the angle between the incident and scattered photons. A second angle (η) defines the scattered photon direction as projected onto a plane perpendicular to the incident photon direction. This angle, which we refer to as the azimuthal scatter angle, is measured from the plane containing the electric vector of the incident photon. For a given value of θ, the scattering cross section for polarized radiation reaches a minimum at $\eta = 0°$ and a maximum at $\eta = 90°$. In other words, photons tend to be scattered at right angles relative to the plane of polarization of the incident radiation. In the case of a Compton scatter polarimeter, this asymmetry, which is maximized for values of θ near 90°, is exploited as a means to determine the linear polarization parameters of the incident radiation.

The successful design of a polarimeter hinges on the ability to reconstruct the kinematics of each event. In this context, we can consider: 1) the ability to measure the energies of both the scattered photon and the scattered electron; and 2) the ability to measure the scattering geometry.

A Compton scatter polarimeter consists of two detectors that are used to measure the energies of both the scattered photon and the scattered electron [2,3]. These measurements also serve to define the scattering geometry. One detector (the *scattering detector*) provides the medium for the Compton interaction to take place. This detector must be designed to maximize the probability of a single Compton interaction with a subsequent escape of the scattered photon. This implies a low-Z material that is sufficiently thick to induce a single Compton scattering, but thin enough to minimize the chance of subsequent interactions. The second detector (the *calorimeter*) absorbs the remaining energy of the scattered photon. Information regarding the scattering geometry comes from the relative location of the detectors. The accuracy with which the scattering geometry can be measured determines the ability to define the modulation pattern and therefore has a direct impact on the polarization sensitivity.

With regard to the definition of the modulation pattern (which follows a $\cos 2\eta$ distribution), it is customary to define, as a figure-of-merit for the polarimeter, the *polarization modulation factor* [2,3]. For a given energy and incidence angle for an incoming photon beam, this can be expressed as,

$$\mu_P = \frac{C_{\max}(P) - C_{\min}(P)}{C_{\max}(P) + C_{\min}(P)} \quad (1)$$

where C_{max} and C_{min} are the maximum and minimum number of counts registered in the polarimeter, respectively, with respect to the azimuthal scatter angle (η). It is useful to define the modulation factor which results from an incident beam that is 100% polarized,

$$\mu_{100} = \frac{C_{\max}(100\%) - C_{\min}(100\%)}{C_{\max}(100\%) + C_{\min}(100\%)} \quad (2)$$

We then use this result, together with the observed modulation factor (μ_P), to determine the level of polarization in a measured beam,

$$P = \frac{\mu_P}{\mu_{100}} = \frac{1}{\mu_{100}} \frac{C_{\max}(P) - C_{\min}(P)}{C_{\max}(P) + C_{\min}(P)} \quad (3)$$

The 3σ sensitivity for measuring polarization is then [2],

$$P(3\sigma) = \frac{3}{\mu_{100} S} \left[\frac{2(S+B)}{T} \right]^{1/2} \quad (4)$$

where S is the source count rate, B is the background count rate, μ_{100} is the modulation factor for 100% polarization and T is the observation time. We see that improved sensitivity to source polarization can be achieved either by increasing the modulation factor (μ_{100}) or by increasing the effective area of the polarimeter (thereby increasing the source count rate).

II. LABORATORY PROTOTYPE

In an earlier paper, we discussed a polarimeter design consisting of a ring of twelve individual scattering detectors (composed of low-Z plastic scintillator) surrounding a single NaI calorimeter [4]. To be recorded as a polarimeter event, an incident photon Compton scatters from one (and only one) of the scattering detectors into the central calorimeter. The incident photon energy can be determined from the sum of the energy losses in both detectors and the azimuthal scattering angle (η) can be determined by the azimuthal angle of the associated scattering detector. When the polarimeter is arranged

so that the incident flux is parallel to the symmetry axis, unpolarized radiation will produce an axially symmetric coincidence rate. If, on the other hand, the incident radiation is linearly polarized, then the coincidence rate will show an azimuthal asymmetry whose phase depends on the position angle of the incident radiation's electric field vector and whose magnitude depends on the degree of polarization. The characteristics of this design were investigated using a series of Monte Carlo simulations that were based on a modified version of the GEANT simulation package.

A prototype of this design was tested in the laboratory, in part to validate our Monte Carlo code [5,6]. For testing purposes, we set up a semicircular array of plastic scintillator elements around a central NaI detector. This semicircular design retained the fundamental physics, but, by eliminating the redundancy, simplified the hardware and associated electronics. A photograph of the laboratory setup is shown in Figure 1.

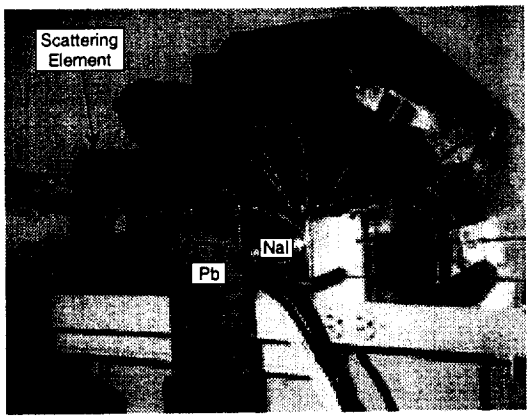

Figure 1: The laboratory prototype showing the plastic scattering elements surrounding the central NaI detector. The lead block was used to shield the NaI detector from direct flux.

A source of polarized photons was generated by Compton scattering photons from a radioactive source [7]. The exact level of polarization is dependent on both the initial photon energy and the photon scatter angle [6,8]. The use of plastic scintillator as a scattering block in generating the polarized beam permits the electronic tagging of the scattered (polarized) photons. This is especially useful in identifying (via coincidence techniques) the interaction of the polarized photons in the polarimeter.

Results from the prototype testing are shown in Figures 2 and 3, where we show the measured data along with Monte Carlo simulation results for two different polarization angles. The polarization values derived from these data agree well with that expected from the laboratory polarization geometry. These results demonstrated: a) the ability of a simple Compton scatter polarimeter to measure hard X-ray polarization; b) the ability of our Monte Carlo code to predict the polarimeter response; and c) the ability to generate a source of polarized photons using a simple scattering technique.

III. Designing a Hard X-Ray Polarimeter

The goal of our program has been to develop a hard X-ray polarimeter that would be suitable for studying solar flare

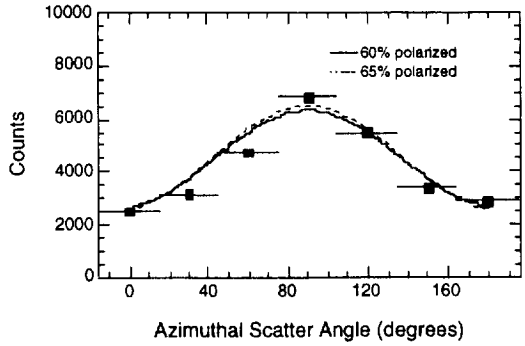

Figure 2: The prototype response to a polarized beam incident on-axis. The smooth curves represent simulation results.

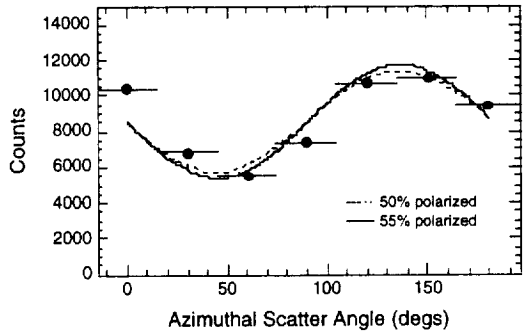

Figure 3: The prototype response to a polarized beam incident on-axis, but with a polarization angle rotated ~45° with respect to that in Figure 4. The smooth curves represent simulation results.

emissions during the upcoming solar maximum. Such a polarimeter must meet the following requirements: 1) it must be compact and light-weight in order to conform with various budget restrictions imposed on any realistic payload; 2) it must be modular in order to provide flexibility as a piggy-back payload and to permit building up an array of detectors with sufficient sensitivity; 3) it must have reasonable detection efficiency over a broad energy range (100–300 keV); and 4) it must have polarization sensitivity below 10% in the 100–300 keV energy range for a moderately-sized (class M5) solar flare. (Based on SMM-GRS observations during the 1980–82 solar maximum, we can expect >50 flares of class M5 or larger during the upcoming solar maximum period.)

A. Design Considerations

There are at least two possible means of improving the polarimeter performance over that of the laboratory prototype: 1) by more precisely measuring the scattering geometry of each event; and 2) by rejecting those events that undergo multiple Compton scattering within the scattering elements. A better geometry definition will serve to more clearly define the modulation pattern of the incident flux. Improved rejection of multiple scatter events will reduce the contribution of such events to the unmodulated component of the polarization response. Our simulations indicate that roughly 30-40% of the events recorded in the prototype polarimeter as valid events involved multiple scattering within a single scatter element.

An improvement in the measured scattering geometry of an event can be achieved by improving the spatial resolution within each detector element. Fully 3-dimensional spatial information is generally not crucial. Since we are principally interested in the azimuthal scattering angle (μ) of each event, spatial information in the x–y plane (i.e., parallel to the front surface of the polarimeter) will be of greatest importance. Although dependent on the precise geometry of the polarimeter, additional information regarding the z–component of the location will generally add little to the information content of the event.

At these energies (100–300 keV), multiple scatter events in the central calorimeter can be safely ignored due to the dominance of the photoelectric effect (assuming that the calorimeter consists of some high-Z inorganic scintillator such as NaI or CsI). Multiple scatter events can be important when the pathlength through the scattering elements becomes comparable to the mean free path of the incident photons (about 6 cm at 100 keV). Since the detection efficiency is, to a great extent, proportional to volume, the geometry of the scattering elements (in terms of both surface area and depth) must be carefully chosen so as to reach a compromise between detection efficiency and the generation of multiple scatter events. If, on the other hand, one can acquire information about the spatial *distribution* of energy deposits, it then becomes possible to distinguish those events with more than one interaction site (i.e., multiple scatter events). Such events can subsequently be rejected during the analysis. This capability would permit the effective use of larger volumes of plastic scintillator, with the potential for a subsequent increase in polarimeter sensitivity. Given the relatively large mean free path of the photons at these energies, a spatial resolution of ~1.0 cm is sufficient to reject a large fraction of the multiple scatter events. Smaller spatial resolutions may be desirable for improving the definition of the scatter geometry.

Two other practical considerations should be noted. In order to reduce accidental coincidences that may be associated with high incident flux levels (such as that from a solar flare), there is a need to shield the calorimeter detectors from direct flux. A thin layer of lead (5 mm thick) is sufficient for this purpose. A second consideration is that of systematic variations in the azimuthal scatter angle distribution due, for example, to detection nonuniformities in the scattering elements. One way to ameliorate this condition is by continuously rotating the polarimeter about its axis of symmetry.

B. A Baseline Polarimeter Design

Based on the above considerations, we have developed a new conceptual design that places an entire device on the front end of a single 5-inch diameter position-sensitive PMT (PSPMT) [6]. Since the focus of our efforts have so far been directed toward solar studies, we refer to this new design as SOLPOL (for SOLar POLarimeter). The design incorporates a array of plastic scintillator elements to provide the improved spatial resolution in the scattering medium and to improve the rejection of multiple scatter events. The plastic elements are arranged in the form of an annulus having an outside diameter of 10 cm (corresponding to the sensitive area of the Hammatsu R3292 5-inch PSPMT). The central portion of the annulus is large enough to insert a small 2 × 2 array of 1 cm CsI scintillators. The CsI scintillators would be coupled to their own read-out devices for the energy measurement and signal timing.

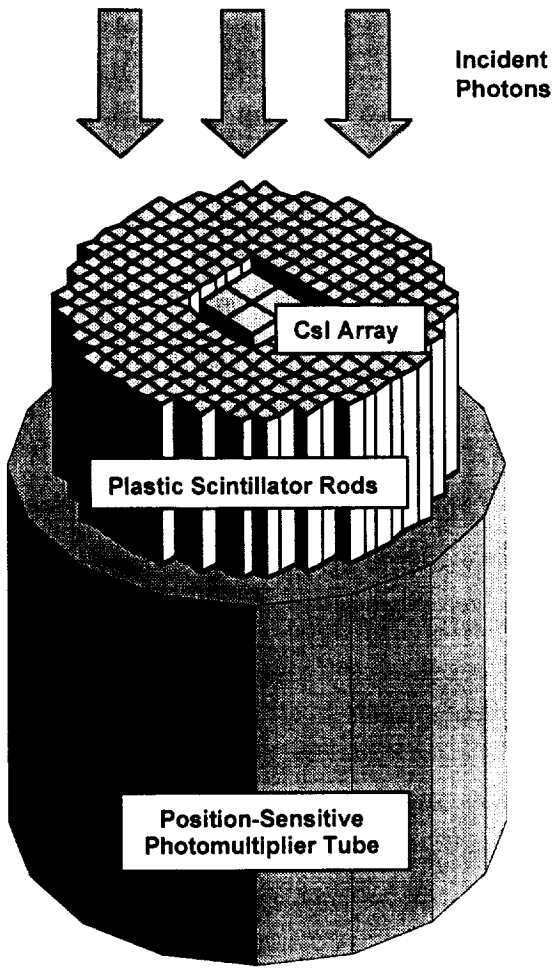

Figure 4: The SOLPOL polarimeter design showing the layout of the plastic scintillator elements and CsI elements on the front surface of a PSPMT. As shown here, the depth of the detector elements is 5.08 cm.

Based on this concept, we have defined the baseline polarimeter design depicted in Figure 4. The scattering medium consists of an array of 5 mm × 5 mm scintillator rods, each with a length of 5.08 cm. The calorimeter medium consists of an array of 1 cm × 1 cm CsI scintillators, each of which also has a length of 5.08 cm. An ideal SOLPOL event is one in which the incident photon Compton scatters in one plastic element, with the remaining photon energy subsequently absorbed in the central CsI array.

We have completed a series of Monte Carlo simulations to determine the charcteristics of this baseline design. These simulations assume that we are able to uniquely identify which plastic scintillator element is involved in the event. The small cross-sectional area of each scintillator element ensures that practically all multiple scatter events are rejected. The energy threshold levels, particularly in the scattering elements, have a significant influence on the performance of the polarimeter at low energies. For the simulations, we have assumed a

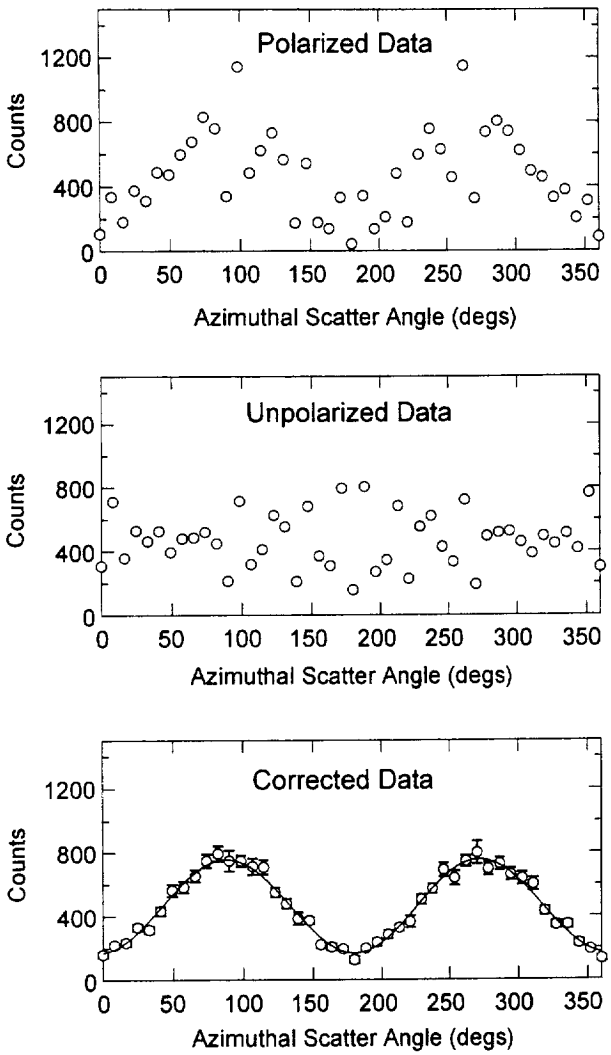

Figure 5: Simulated polarimeter data showing how the measured data is corrected for intrinsic geometric effects to extract the true modulation pattern. These data correspond to the response of the baseline SOLPOL design to a monoenergetic beam of 150 keV photons incident at 0°.

threshold energy of 15 keV in both the plastic and CsI scintillators.

Figure 5 illustrates the nature of the SOLPOL data. In this case, the data are from Monte Carlo simulations using the baseline SOLPOL design (Figure 4). The first panel shows the polarization response to a fully polarized monoenergetic beam of 150 keV photons vertically incident on the front surface of the polarimeter. This distribution includes not only the intrinsic modulation pattern due to the Compton scattering process, but it also includes geometric effects related to the specific layout of the detector elements within the polarimeter and the associated quantization of possible scatter angles. The geometric effects can be more clearly seen in the case of an incident beam that is completely unpolarized, as shown in the second panel of Figure 5. (In practice, for analyzing real data, this unpolarized distribution would be determined by smulations rather than by direct measurements.) To extract the true distribution of polarized events, we divide the polarized distribution by the unpolarized distribution and normalize by the average of the unpolarized distribution. Only when we correct the raw data in this fashion do we clearly see the cos 2η modulation pattern that is expected (the third panel of Figure 5).

Simulated data have also been used to evaluate the performance characteristics of the baseline design. Figures 6 and 7 show the effective area and modulation factor, respectively, as a function of incident photon energy. In both cases, are shown the results for two different detector depths – 5.08 cm (as depicted in Figure 4) and 7.62 cm. Although the deeper detector clearly presents an advantage in terms of effective area, the varying detector depth appears to have little influence on the modulation factor. In practice, the advantage of increased effective area for a deeper detector must be offset by the decrease in light collection efficiency and the consequent effects on the detector threshold (Figure 11).

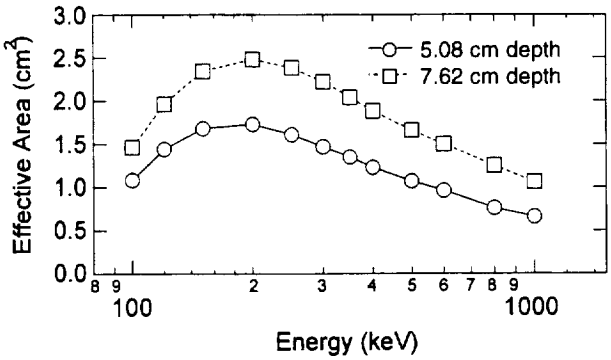

Figure 6: The effective area as a function of energy for the baseline design having a depth of both 5.08 cm and 7.62 cm.

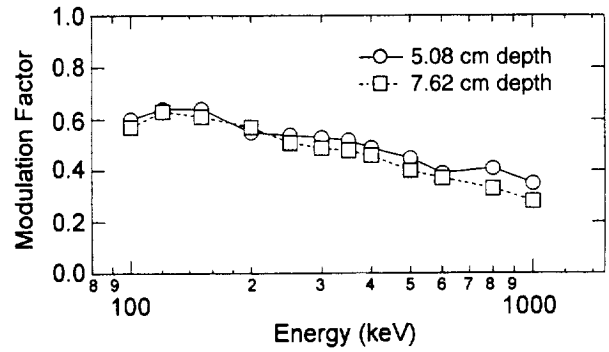

Figure 7: The modulation factor as a function of energy for the baseline design having depths of 5.08 cm and 7.62 cm.

One potentially useful aspect of the SOLPOL design is that there exists a significant polarization response at large off-axis angles. This can be seen in Figure 8, which is based on simulations with a detector depth of 5.08 cm. The effective area remains relatively constant at large angles. This results from the fact that the exposed geometric area of the detector remains relatively constant. Although there is a significant decrease in the modulation factor at large angles, there is still significant polarization response even at 60° incidence angle. The off-axis response of this design would be very useful, for example, in studies of gamma-ray bursts.

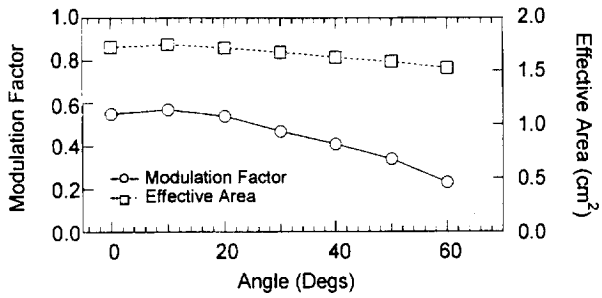

Figure 8: The modulation factor and effective area at 200 keV for various incidence angles. The polarimeter maintains good response out to 60° incidence angles.

IV. Science Model Development

Our recent work has concentrated on the fabrication of a science model based on the baseline SOLPOL design (Figure 4). Although the fabrication of the science model is not yet complete, we have made progress in several key technical areas.

A. PSPMT Imaging Tests

Our intial design incorporated the use of scintillating fibers as a scattering medium [6]. This choice was motivated by the fine (sub-mm) spatial resolution that could, in principle, be achieved. We have assembled and tested a PSPMT / fiber-bundle module for the purpose of evaluating the imaging characteristics of such a device. The Bicron fiber bundle consisted of an 11 × 11 array of 3˝ long fibers, each with a cross-sectional area of 5 × 5 mm^2. The scintillating core of each fiber was based on BCF-10 scintillator. In addition to the standard PMMA cladding, each fiber was coated with an extramural absorber to reduce cross-talk between fibers. The fibers were viewed from one end by a 3˝ square Hamamatsu R2487 PSPMT. Signal readout from the PSPMT was provided by a charge-divsion circuit. Readout of each event was triggered by a signal from the last dynode. The data processing and acquisition was achieved using a combination of NIM and CAMAC modules, with the final data recorded via a SCSI interface to a Power Macintosh computer running Kmax software.

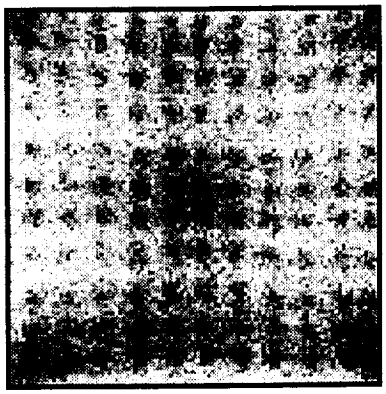

Figue 9: Fiber bundle flood test map based on uniform irradiance by 122 keV photons from ^{57}Co. The individual fiber elements (each 5 × 5 mm^2) can be clearly discerned.

Figure 9 shows the distribution of measured events resulting from a uniform irradiation of the front surface of the fiber bundle by 122 keV photons from ^{57}Co. The array of fibers is clearly defined. Also evident is the nonuniform nature of the PSPMT response.

The response of the PSPMT / fiber bundle module to a collimated beam of 662 keV photons is shown in Figure 12. The beam spot in this case was ~3-4 mm. The spatial response is dominated by a single fiber and its nearest neighbors. This suggests that individual events can be located with an accuracy comparable to the size of the plastic elements.

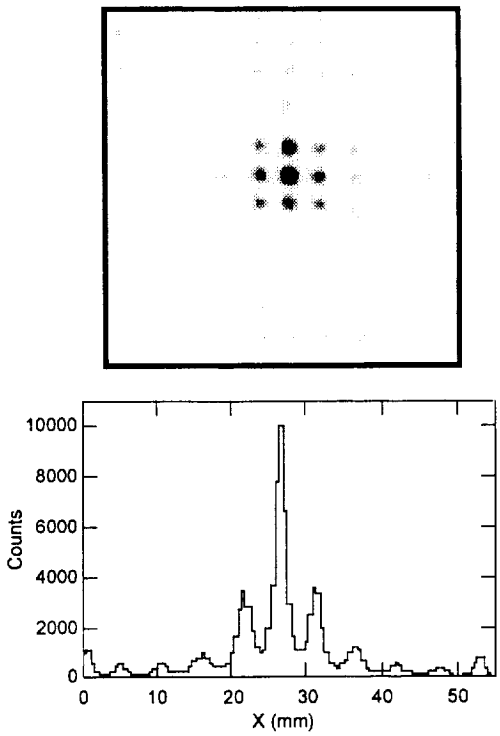

Figure 10: Distribution of events in the fiber bundle when irradiated with a collimated beam of 662 keV photons from ^{137}Cs. (Beam spot size ~3-4 mm.)

B. Light Output of Scattering Elements

The initial decision to use scintillating fibers led to a concern about the light collection efficiency and its potential impact on the energy threshold. Our ultimate goal is to achieve a polarimeter energy threshold of 50 keV. This requires a scattering element energy threshold of 15 keV. A major concern was whether such a low threshold energy could be achieved with scintillating fibers. Given the relatively large cross-sectional area that we were considering for the fibers, one potentially better alternative would be the use of individual plastic scintillating rods.

Motivated by these concerns, we made several laboratory measurements to determine the relative light output of scintillating fibers as compared to standard pieces of plastic scintillator. Specifically, we tested the light output of individual plastic scintillating rods with the same cross-sectional area (5 × 5 mm^2) as our scintillating fibers, but of varying lengths (2.54 cm, 5.08 cm and 7.62 cm). The (Bicron BC-404) scintilator rods were individually wrapped in white plumbers tape to provide optical isolation and assembled into a

4 × 4 array. Tests were performed using a (non-imaging) 2" (5.08 cm) PMT (EMI 9755NA).

The results of our testing with a ^{133}Ba source are shown in Figure 11. The relative light output of the various assemblies can be judged by the location of the Compton edge, which results primarily from 356 keV photons interacting in the scintillator. These data show that the shorter geometries provide for greater light collection efficiency. More importantly, for the same (3") geometry, the light output of the individual scintillator rods is about a factor of 2.5 times the light output of the scintillating fibers. Although scintillating fibers might be preferred for very small cross sectional areas (ease of fabrication) or for very long geometries (light propagation), *these results clearly argue in favor of using an array of individual plastic scintillator rods, rather than a scintillating fiber bundle.*

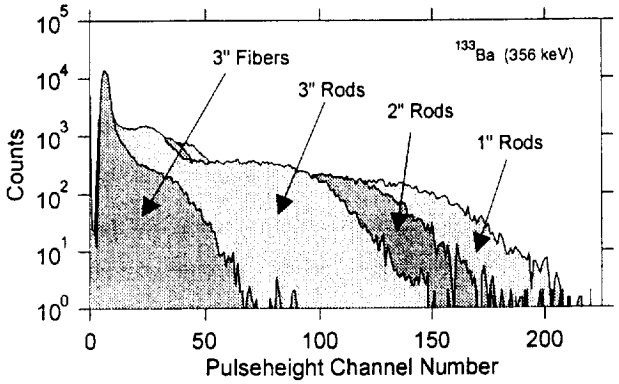

Figue 11: Spectra from ^{133}Ba recorded for different scintillator assemblies (of varying lengths) and for a scintillating fiber bundle. In all cases, the individual elements (or fibers) were 5 × 5 mm^2. The relative light output of the scintillator assemblies is clearly superior to that of the scintillating fibers.

C. Recent Progress

We are presently working on the fabrication of the SOLPOL science model. The wrapping of 280 individual plastic scintillator elements has recently been completed. The final asembly and initial testing should take place early in 1999. Our initial imaging results using a bundle of these elements coupled to a 5" PSPMT are comparable to the results we achieved with the fiber bundle. The goals of these tests will be to evaluate the light output and spatial resolution of the scintillator array and to demonstrate the basic polarimetric capabilities of the device

For the initial science model fabrication, we have chosen a plastic element depth of 2". This will provide a reasonable level of light output, while retaining a large detection efficiency. (Further studies will be required to determine an optimum depth based on light output and detection efficiency considerations.) For the calorimeter elements, we will use an array of 1 cm × 1 cm CsI elements coopled to a Hamamatsu R5900-04 multi-anode PMT (MAPMT).

The initial tests will make use of the four readouts from a charge division network as supplied by Hammamatsu. This will provide a weighted average of the spatial distribution of the measured light output. Later tests will seek to make more effective use of the full spatial information afforded by the PSPMT using signals from the individual PSPMT anode wires. The R3292 PSPMT is designed with 28(X) plus 28(Y) cross-wire anodes. Rather than using all 56 individual channels, we plan to simplify the readout using only fourteen (7x, 7y) anode wire sections. Other workers have succeeded in resolving individual 3mm YAP crystal elements using such a readout scheme and a center-of-gravity calculation for determining the interaction location [9]. The utility of this readout scheme for rejecting multiple scatter events will be investigated. If needed, we will more fully configure the PSPMT to test the multiple scatter event rejection at finer spatial scales. However, given the mean free path of photons in the plastic (6 cm at 100 keV), we expect that a high level of multiple scatter event rejection can be achieved with the fourteen channel readout scheme.

In the future we may decide to explore alternative readout schemes. Despite the increased cost and complexity of having a large number of individual channels (one per detector element), the technical advantages may dictate such a course of development. Our science model testing will help us to evaluate the need for such alternative technologies

V. SUMMARY

The goal of these science model tests is to verify the performance characteristics of the SOLPOL design and to define the final electronics configuration. Once this has been accomplished, we can move forward with the detailed design and fabrication of a self-contained engineering model. We anticipate that this design would be used in the context of an array of polarimeter modules. For solar flares, we calculate that an array of 4 modules is capable of measuring sensitivity levels down to a few percent in X-class flares. A larger array of 16 modules would be capable of measuring solar flare polarization levels below 1% for the largest events and would also be capable of measuring polarization levels down to about 15% in some of the largest γ-ray bursts [5]. Although similar designs have been discussed in the literature [10,11], we are unaware of any other *active* effort to specifically measure polarization in solar flares or in γ-ray bursts at energies above 100 keV.

In addition to its potential for studying transient sources, the SOLPOL design might also be useful in the context of an imaging polarimeter. For example, a SOLPOL element or array of elements could be used with a rotation modulation collimator to achieve arc-second angular resolution. Such an approach is not unlike that employed for hard X-ray imaging (without polarization capability) in the upcoming HESSI mission. The spatial information intrinsic to the SOLPOL design might also be useful in a coded-aperture system, although perhaps limited to arc-minute angular resolutions. We have recently embarked on an effort to evaluate the various possible imaging techniques that could be used with a SOLPOL-like device.

VI. ACKOWLEDGEMENT

This work has been supported by NASA grants NAGW-5704 and NAG5-7294.

VII. REFERENCES

[1] R.D. Evans, The Atomic Nucleus, New York: McGraw-Hill, 1958.

[2] R. Novick, "Stellar and solar X-ray polarimetry," *Space Science Reviews*, vol. 18, pp. 389-408, 1975.

[3] F. Lei, A.J. Dean and G.L. Hills, "Compton scatter polarimetry in gamma-ray astronomy," *Space Science Reviews*, vol. 82, pp. 309-388, 1997.

[4] M. McConnell, D. Forrest, K. Levenson, and W.T. Vestrand, "The design of a gamma-ray burst polarimeter," in AIP Conf. Proc. 280, *Compton Gamma-Ray Observatory*, M. Friedlander, N. Gehrels and D.J. Macomb, Eds. New York: AIP, 1993, pp. 1142-1146.

[5] M.L. McConnell, D.J. Forrest, J. Macri, J.M. Ryan, and W.T. Vestrand, "Development of a hard X-ray polarimeter for gamma-ray bursts," AIP Conf. Proc. 428, *Gamma-Ray Bursts*, C.A. Meegan and P. Cushman, Eds. New York: AIP, 1998, pp. 889-893.

[6] M.L. McConnell, D.J. Forrest, J. Macri, M. McClish, M. Osgood, J.M. Ryan, W.T. Vestrand and C. Zanes "Development of a hard X-ray polarimeter for solar flares and gamma-ray bursts," *IEEE Trans. Nucl. Sci.*, vol. 45, no. 3, pp. 910-914, June, 1998.

[7] H. Sakurai, M. Noma, and H. Niizeki, "A hard x-ray polarimeter utilizing Compton scattering," in *SPIE Conf. Proc.*, vol. 1343, pp.512-518, 1990.

[8] W.H. McMaster, "Matrix representation of polarization," *Reviews of Mod. Phys.*, vol. 33, no. 1, pp. 8-28, January 1961.

[9] R. Wojcik, S. Majewski, B. Kross, D. Steinbach, and A.G., "High spatial resolution gamma imaging detector based on a 5" diameter R3292 Hamamatsu PSPMT," *IEEE Trans. Nucl. Sci.*, vol. 45, no. 3, pp. 487-491, June, 1998.

[10] G. Chanan, A.G. Emslie, and R. Novick, "Prospects for solar flare X-ray polarimetry," *Solar Physics*, vol. 118, pp. 309-319, 1988.

[11] T.L. Cline, et al., "A gamma-ray burst polarimeter study," in *Proceedings of the 25th Internat. Cosmic Ray Conf.*, vol. 5, pp. 25-28, 1997.

to be published in Proc. SPIE (1999)

Recent Laboratory Tests of a Hard X-Ray Solar Flare Polarimeter

M.L. McConnell*, J.R. Macri, M. McClish and J. Ryan

Space Science Center, Morse Hall, University of New Hampshire, Durham, New Hampshire 03824

ABSTRACT

We report on the development of a Compton scatter polarimeter for measuring the linear polarization of hard X-rays (50-300 keV) from solar flares. Such measurements would be useful for studying the directivity (or beaming) of the electrons that are accelerated in solar flares. We initially used a simple prototype polarimeter to successfully demonstrate the reliability of our Monte Carlo simulation code and to demonstrate our ability to generate a polarized photon source in the lab. We have recently fabricated a science model based on a modular design concept that places a self-contained polarimeter module on the front-end of a 5-inch position-sensitive PMT (PSPMT). The PSPMT is used to determine the Compton interaction location within an annular array of small plastic scintillator elements. Some of the photons that scatter within the plastic scintillator array are subsequently absorbed by a small centrally-located array of CsI(Tl) crystals that is read out by an independent multi-anode PMT. The independence of the two PMT readout schemes provides appropriate timing information for event triggering. We are currently testing this new polarimeter design in the laboratory to evaluate the performance characteristics of this design. Here we present the initial results from these laboratory tests. The modular nature of this design lends itself toward its accomodation on a balloon or spacecraft platform. A small array of such modules can provide a minimum detectable polarization (MDP) of less than 1% in the integrated 50-300 keV energy range for X-class solar flares.

Keywords: Hard X-Rays, Polarimetry, Solar Flares, Gamma-Ray Bursts, PSPMT

1. INTRODUCTION

The basic physical process used to measure linear polarization of hard X-rays (50–300 keV) is Compton scattering.[1] In general, the scattering geometry can be described by two angles. The first of these is the *Compton scatter angle* (θ), the angle between the incident and scattered photons. A second angle (η) defines the scattered photon direction as projected onto a plane perpendicular to the incident photon direction. This angle, which we refer to as the *azimuthal scatter angle*, is measured from the plane containing the electric vector of the incident photon. For a given value of θ, the scattering cross section for polarized radiation reaches a minimum at $\eta = 0°$ and a maximum at $\eta = 90°$. In other words, photons tend to be Compton scattered at right angles relative to the plane of polarization of the incident radiation. In the case of a Compton scatter polarimeter, this asymmetry, which is maximized for values of θ near 90°, is exploited as a means to determine the linear polarization parameters of the incident radiation. The successful design of a polarimeter hinges on the ability to reconstruct the kinematics of each event. In this context, we can consider: 1) the ability to measure the energies of both the scattered photon and the scattered electron; and 2) the ability to measure the scattering geometry.

A Compton scatter polarimeter consists of two detectors that are used to measure the energies of both the scattered photon and the scattered electron.[2, 3] These measurements also serve to define the scattering geometry. One detector (the *scattering detector*) provides the medium for the Compton interaction to take place. This detector must be designed to maximize the probability of a single Compton interaction with a subsequent escape of the scattered photon. This implies a low-Z material that is sufficiently thick to induce a single Compton scattering, but thin enough to minimize the chance of subsequent interactions. The second detector (the *calorimeter*) absorbs the remaining energy of the scattered photon. Information regarding the scattering geometry comes from the relative location of the detectors. Knowledge of the scattering geometry can be further improved by measuring the interaction location *within* each detector. The accuracy with which the scattering geometry can be measured determines the ability to define the modulation pattern and therefore has a direct impact on the polarization sensitivity.

* Correspondence: E-mail: Mark.McConnell@unh.edu

With regard to the definition of the modulation pattern (which follows a cos 2η distribution), it is customary to define, as a figure-of-merit for the polarimeter, the *polarization modulation factor*.[2] For a given energy and incidence angle of an incoming photon beam, this can be expressed as,

$$\mu_P = \frac{C_{\max}(P) - C_{\min}(P)}{C_{\max}(P) + C_{\min}(P)} \tag{1}$$

where C_{max} and C_{min} are the maximum and minimum number of counts registered in the polarimeter, respectively, with respect to the azimuthal scatter angle (η). It is useful to define the modulation factor which results from an incident beam that is 100% polarized,

$$\mu_{100} = \frac{C_{\max}(100\%) - C_{\min}(100\%)}{C_{\max}(100\%) + C_{\min}(100\%)} \tag{2}$$

We then use this result (often derived from Monte Carlo simulations), together with the observed modulation factor (μ_P), to determine the level of polarization in a measured beam,

$$P = \frac{\mu_P}{\mu_{100}} = \frac{1}{\mu_{100}} \frac{C_{\max}(P) - C_{\min}(P)}{C_{\max}(P) + C_{\min}(P)} \tag{3}$$

The 3σ sensitivity for measuring polarization is then,[2]

$$P(3\sigma) = \frac{3}{\mu_{100} S} \left[\frac{2(S+B)}{T} \right]^{1/2} \tag{4}$$

where S is the source count rate, B is the background count rate, μ_{100} is the modulation factor for 100% polarization and T is the observation time. We see that improved sensitivity to source polarization can be achieved either by increasing the modulation factor (μ_{100}) or by increasing the effective area of the polarimeter (thereby increasing the source count rate).

2. LABORATORY PROTOTYPE

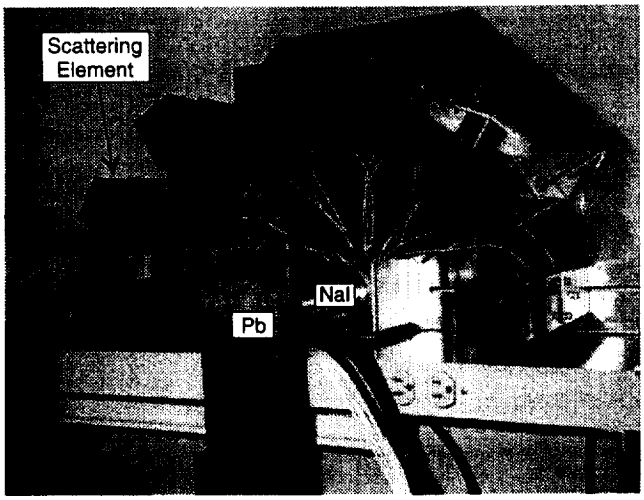

Figure 1: The laboratory prototype showing the plastic scattering elements surrounding the central NaI detector. A lead block was used to shield the NaI detector from direct flux.

In our earliest work, we discussed a simple polarimeter design consisting of a ring of twelve individual scattering detectors (composed of low-Z plastic scintillator) surrounding a single NaI calorimeter.[4] To be recorded as a polarimeter event, an incident photon Compton scatters from one (and only one) of the scattering detectors into the central calorimeter. The incident photon energy can be determined from the sum of the energy losses in both detectors. The azimuthal scattering angle (η) can be determined by the azimuthal angle of the associated scattering detector. When the polarimeter is arranged so that the incident flux is parallel to the symmetry axis, unpolarized radiation will produce an axially symmetric coincidence rate. If, on the other hand, the incident radiation is linearly polarized, then the coincidence rate will show an azimuthal asymmetry whose phase depends on the position angle of the incident radiation's electric field vector and whose magnitude depends on the degree of polarization. The characteristics of this design were investigated using a series of Monte Carlo simulations that were based on a modified version of the GEANT simulation package.

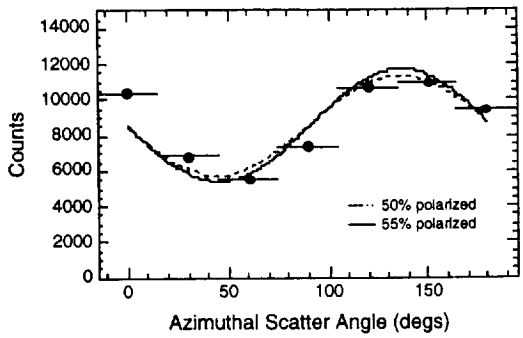

Figure 3: The prototype response to a polarized beam incident on-axis, but with a polarization angle rotated ~45° with respect to that in Figure 4. The smooth curves represent simulation results.

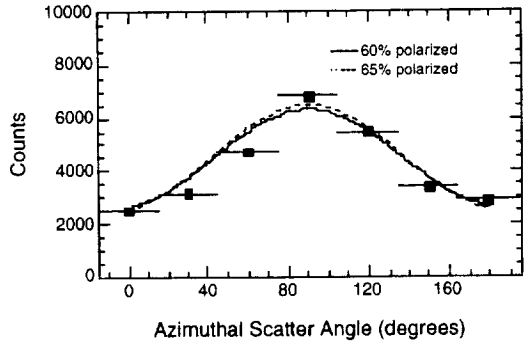

Figure 2: The prototype response to a polarized beam incident on-axis. The smooth curves represent simulation results.

A prototype of this design was tested in the laboratory, in part to validate our Monte Carlo code.[5, 6] For testing purposes, we set up a semicircular array of plastic scintillator elements around a central NaI detector. This semicircular design retained the fundamental physics, but, by eliminating the redundancy, simplified the hardware and associated electronics. A photograph of the laboratory setup is shown in Figure 1. A source of polarized photons was generated by Compton scattering photons from a radioactive source.[7] The exact level of polarization of such a scattered photon beam is dependent on both the initial photon energy and the photon scatter angle.[6, 8] The use of plastic scintillator as a scattering block in generating the polarized beam permits the electronic tagging of the scattered (polarized) photons. This is especially useful in identifying (via coincidence techniques) the interaction of the polarized photons in the polarimeter.

Results from the prototype testing are shown in Figures 2 and 3, where we show the measured data along with Monte Carlo simulation results for two different polarization angles. The polarization values derived from these data agree well with that expected from the laboratory polarization geometry. These results demonstrated: a) the ability of a simple Compton scatter polarimeter to measure hard X-ray polarization; b) the ability of our Monte Carlo code to predict the polarimeter response; and c) the ability to generate a source of polarized photons using a simple scattering technique.

3. DESIGNING A HARD X-RAY POLARIMETER

The goal of our program has been to develop a hard X-ray polarimeter that would be suitable for studying solar flare emissions. Such a polarimeter must meet the following requirements: 1) it must be compact and light-weight in order to conform with various budget restrictions imposed on any realistic payload; 2) it must be modular in order to provide flexibility as a piggy-back payload and to permit building up an array of detectors with sufficient sensitivity; 3) it must have reasonable detection efficiency over a broad energy range (50–300 keV); and 4) it must have polarization sensitivity below 10% in the 50–300 keV energy range for a moderately-sized (class M5) solar flare. (Based on SMM-GRS observations during the 1980–82 solar maximum, we can expect >50 flares of class M5 or larger during the upcoming solar maximum period.)

3.1. Design considerations

There are at least two possible means of optimizing the performance of a Compton scatter polarimeter: 1) by more precisely measuring the scattering geometry of each event; and 2) by rejecting those events that undergo multiple Compton scattering within the scattering elements. A better geometry definition will serve to more clearly define the modulation pattern of the incident flux. Improved rejection of multiple scatter events will reduce the contribution of such events to the unmodulated component of the polarization response.

An improvement in the measured scattering geometry of an event can be achieved by improving the spatial resolution within each detector element. Fully 3-dimensional spatial information is generally not crucial. Since we are principally interested in the azimuthal scattering angle (μ) of each event, spatial information in the x–y plane (i.e., parallel to the front surface of the

polarimeter) will be of greatest importance. Although dependent on the precise geometry of the polarimeter, additional information regarding the z–component of the location will generally add little to the information content of the event.

At these energies (50–300 keV), multiple scatter events in the central calorimeter can be safely ignored due to the dominance of the photoelectric effect (assuming that the calorimeter consists of some high-Z inorganic scintillator such as NaI or CsI). Multiple scatter events can be important when the pathlength through the scattering elements becomes comparable to the mean free path of the incident photons (about 6 cm at 100 keV). Since the detection efficiency is, to a great extent, proportional to volume, the geometry of the scattering elements (in terms of both surface area and depth) must be carefully chosen so as to reach a compromise between detection efficiency and the generation of multiple scatter events. If, on the other hand, one can acquire information about the spatial *distribution* of energy deposits, it then becomes possible to distinguish those events with more than one interaction site (i.e., multiple scatter events). Such events can subsequently be rejected during the analysis. This capability would permit the effective use of larger volumes of plastic scintillator, with the potential for a subsequent increase in polarimeter sensitivity. Given the relatively large mean free path of the photons at these energies, a spatial resolution of ~1.0 cm is sufficient to reject a large fraction of the multiple scatter events. Smaller spatial resolutions may be desirable for improving the definition of the scatter geometry.

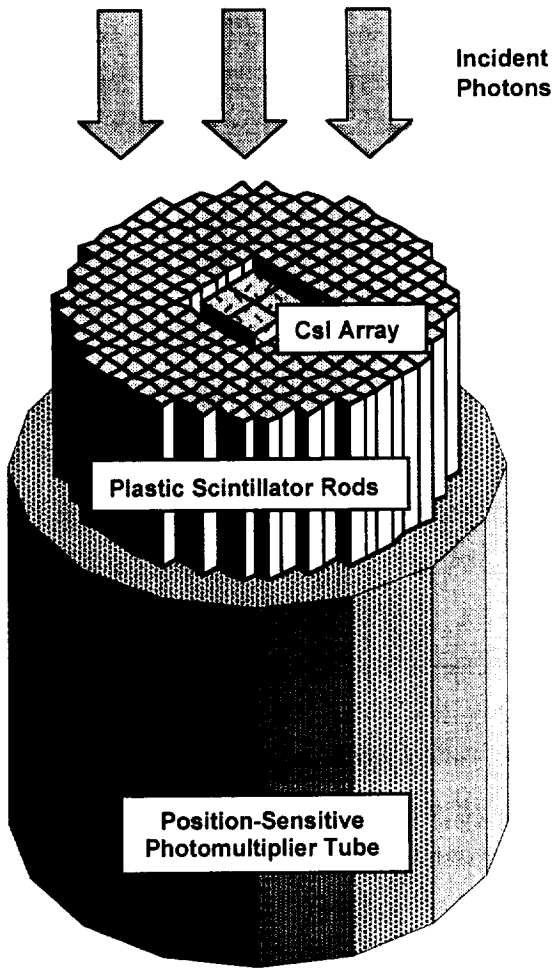

Figure 4: The SOLPOL polarimeter design showing the layout of the plastic scintillator elements and CsI(Tl) elements on the front surface of a PSPMT. Not shown here is the 4-element multianode PMT used for readout of the CsI(Tl) array and the lead shield that would be used to block direct flux from the CsI(Tl) array.

Two other practical considerations should be noted. In order to reduce accidental coincidences that may be associated with high incident flux levels (such as that from a solar flare), there is a need to shield the calorimeter detectors from direct flux. A thin layer of lead (5 mm thick) is sufficient for this purpose. A second consideration is that of systematic variations in the azimuthal scatter angle distribution due, for example, to detection nonuniformities in the scattering elements. One way to ameliorate this condition is by continuously rotating the polarimeter about its axis of symmetry.

3.2. A Modular Polarimeter Design

Based, in part, on the above considerations, we have developed a modular polarimeter design that places an entire device on the front end of a single 5-inch diameter position-sensitive PMT (PSPMT).[6,9] Since the focus of our efforts has so far been directed toward solar studies, we refer to this new design as SOLPOL (for SOLar POLarimeter). The design incorporates an array of plastic scintillator elements to provide the improved spatial resolution in the scattering medium and to improve the rejection of multiple scatter events. Each plastic scintillator element is optically-isolated with a cross sectional area of 5 × 5 mm^2. The plastic elements are arranged in the form of an annulus having an outside diameter of 10 cm (corresponding to the sensitive area of the Hammatsu R3292 5-inch PSPMT). The central portion of the annulus is large enough to insert a small 2 × 2 array of 1 cm CsI(Tl) scintillators. The CsI(Tl) scintillators are coupled to their own independent multi-anode PMT (MAPMT) for the energy measurement and signal timing. In the baseline design, depicted in Figure 4, both the plastic and CsI(Tl) elements have a depth of 5 cm. An ideal SOLPOL event is one in which the incident photon Compton scatters in one plastic element, with the remaining photon energy subsequently absorbed in the central CsI array.

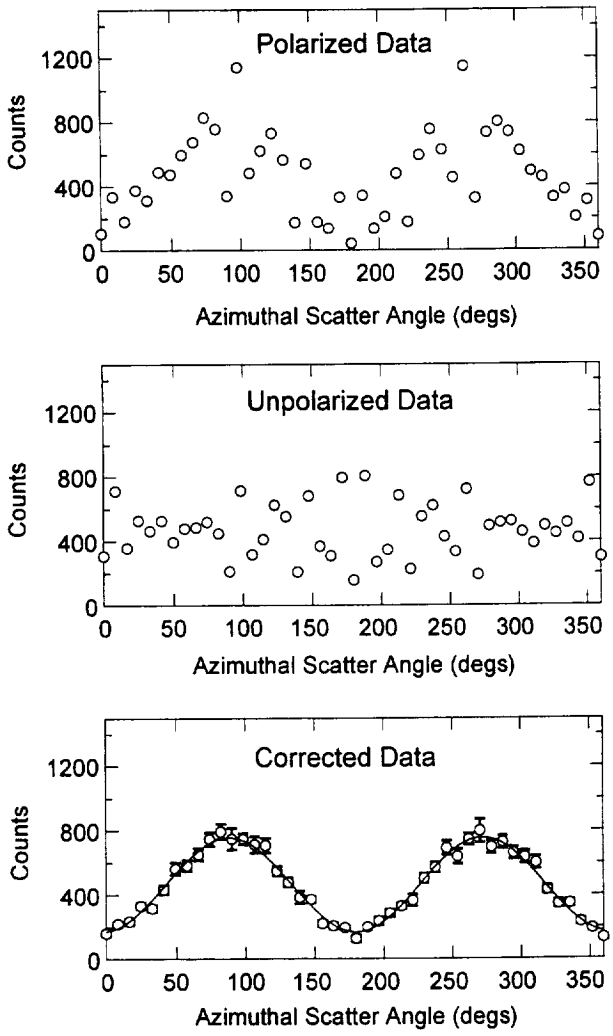

Figure 5: Simulated polarimeter data showing how the measured data is corrected for intrinsic geometric effects to extract the true modulation pattern. These data correspond to the response of the baseline SOLPOL design to a monoenergetic beam of 150 keV photons incident at 0°.

We have completed a series of Monte Carlo simulations to determine the charcteristics of this design. These simulations assume that we are able to uniquely identify which plastic scintillator element is involved in the event. The small cross-sectional area of each scintillator element ensures that practically all multiple scatter events are rejected. The energy threshold levels, particularly in the scattering elements, have a significant influence on the performance of the polarimeter at low energies. For the simulations, we have assumed a threshold energy of 15 keV in both the plastic and CsI scintillators.

Figure 5 illustrates the nature of the SOLPOL data. In this case, the data are from Monte Carlo simulations using the baseline SOLPOL design (Figure 4). The first panel shows the polarization response to a fully polarized monoenergetic beam of 150 keV photons vertically incident on the front surface of the polarimeter. This distribution includes not only the intrinsic modulation pattern due to the Compton scattering process, but it also includes geometric effects related to the specific layout of the detector elements within the polarimeter and the associated quantization of possible scatter angles. The geometric effects can be more clearly seen in the case of an incident beam that is completely unpolarized, as shown in the second panel of Figure 5. (In practice, for analyzing real data, this unpolarized distribution would be determined by simulations rather than by direct measurements.) To extract the true distribution of polarized events, we divide the polarized distribution by the unpolarized distribution and normalize by the average of the unpolarized distribution. Only when we correct the raw data in this fashion do we clearly see the cos 2η modulation pattern that is expected (the third panel of Figure 5).

Simulated data have also been used to evaluate the performance characteristics of the baseline design. Figures 6 and 7 show the effective area and modulation factor, respectively, as a function of incident photon energy. In

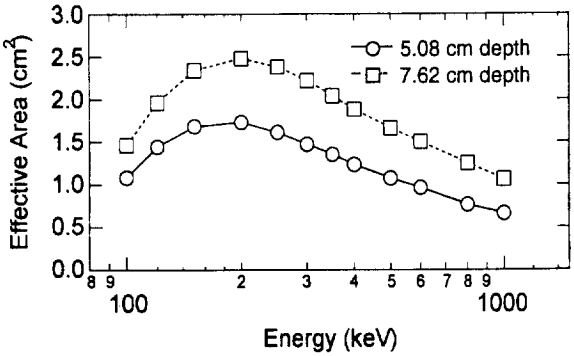

Figure 6: The effective area as a function of energy for the baseline design having a depth of both 5.08 cm and 7.62 cm.

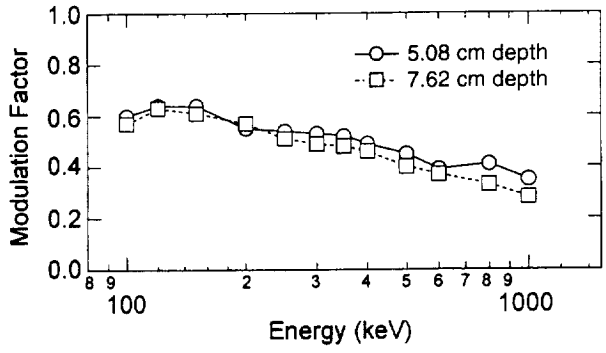

Figure 7: The modulation factor as a function of energy for the baseline design having depths of 5.08 cm and 7.62 cm.

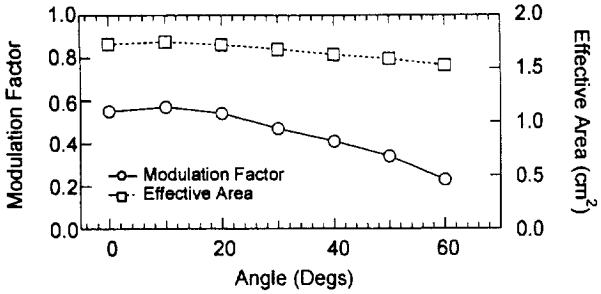

Figure 8: The modulation factor and effective area at 200 keV for various incidence angles. The polarimeter maintains good response out to 60° incidence angles.

both cases, are shown the results for two different detector depths – 5.08 cm (as depicted in Figure 4) and 7.62 cm. Although the deeper detector clearly presents an advantage in terms of effective area, the varying detector depth appears to have little influence on the modulation factor. In practice, the advantage of increased effective area for a deeper detector must be offset by the increase in background as well as the decrease in light collection efficiency (with its consequent effects on the detector threshold).

One potentially useful aspect of the SOLPOL design is that there exists a significant polarization response at large off-axis angles. This can be seen in Figure 8, which is based on simulations with a detector depth of 5.08 cm. The effective area remains relatively constant at large angles. This results from the fact that the exposed geometric area of the detector remains relatively constant. Although there is a significant decrease in the modulation factor at large angles, there is still significant polarization response even at 60° incidence angle. The off-axis response of this design would be very useful, for example, in studies of gamma-ray bursts.

4. SCIENCE MODEL FABRICATION AND TESTING

We have recently completed the fabrication of a science model based on the modular SOLPOL design. The plastic scintillator array is composed of individual pieces of Bicron BC-404 scintillator. Each 5 mm × 5 mm × 50 mm scintillator element is individually wrapped in Tyvek® to maximize light collection efficiency and to provide optical isolation. A thin layer of Kapton® tape was then used to hold the wrapping in place. A thin aluminum housing encloses both the PSPMT and the plastic scintillator array. The calorimeter detector assembly is a 2 × 2 array of 1 cm CsI(Tl) elements coupled to a MAPMT (Hamamatsu R5900 with a 2 × 2 anode array) and enclosed within its own, separate light-tight housing. During operations, the calorimeter detector assembly is inserted into a central well in the PSPMT / plastic scintillator housing. Data processing and acquisition is achieved using a combination of NIM and CAMAC modules, with the final data recorded via a SCSI interface on a Macintosh computer.

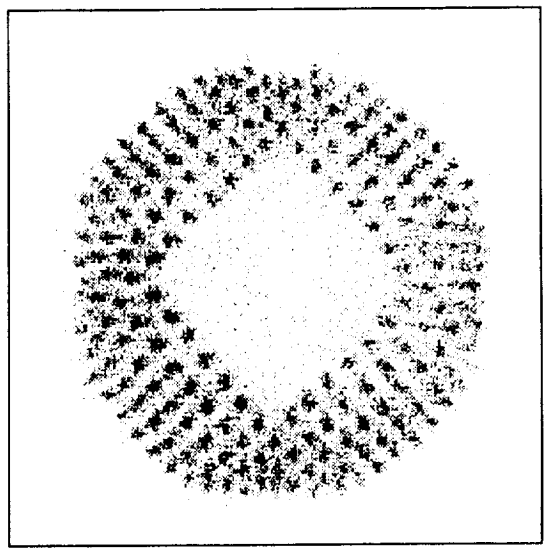

Figure 9: Distribution of measured polarimeter events within the plastic array. These are events (from ^{137}Cs) which scatter between the plastic elements and the central calorimeter. The spatial resolution of the PSPMT cleatly distinguishes individual 5mm plastic elements.

The initial laboratory tests make use of a charge division network for the PSPMT (Hammamatsu R3292) that provides a weighted average of the spatial distribution of the measured light output using only four signals (two signals in x and 2 signals in y). In principle, more precise information regarding the distribution of energy deposits within the plastic arrays can be derive from using all 56 (28-x plus 28-y) anode signals from the PSPMT. We first plan to pursue an intermediate approach using only fourteen (7-x plus 7-y) anode wire sections. Such an approach has succeeded in resolving individual 3mm YAP crystal elements using a center-of-gravity calculation for determining the interaction location.[10] The utility of this readout scheme for rejecting multiple scatter events will be investigated. Given the mean free path of photons in plastic (6 cm at 100 keV), we expect that a high level of multiple scatter event rejection can be achieved with the fourteen channel readout scheme, thus minimizing the required number of electrical channels. If needed, we will more fully configure the PSPMT to test the multiple scatter event rejection at finer spatial scales.

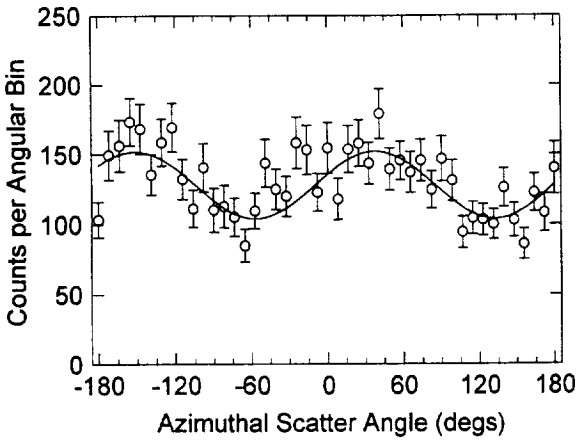

Figure 10: The azimuthal scatter distribution for the baseline run with the SOLPOL science model.

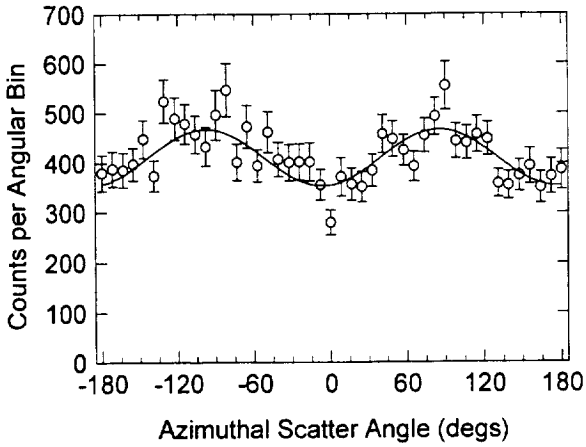

Figure 11: The azimuthal scatter distribution for a run with the SOLPOL science model. In this case the plane of polarization was shifted by ~45° with respect to that in Figure 10.

Figure 9 shows the spatial distribution of Compton scatter locations within the plastic scintillator array. Unpolarized photons from a ^{137}Cs source were used to directly illuminate the front surface of the polarimeter. Only events that were coincident between the plastic array and the central CsI(Tl) were recorded. The individual 5 mm plastic elements are clearly resolved by the PSPMT. These data suggest that even smaller elements could be used with this PSPMT. Also evident in the event distribution is the central well of the plastic array in which the calorimeter detector assembly is located.

Preliminary results of the science model response to a polarized laboratory beam have recently been obtained. These tests employed the use of a tagged polarized photon beam, as described in section 2. The analysis is limited in that the runs are of limited duration (poor event statistics), the spatial information within the calorimeter array is not yet utilized, and a proper energy calibration for each detector component is not yet available to optimize the event selection. A quantitative analysis of the polarimetric response is therefore not yet possible. Nonetheless, we have been able to demonstrate the existence of a polarization signal. This is seen in Figures 10 and 11, which show the azimuthal modulation of the scattered photon events at two different polarization angles offset by ~45°. In each case, the curve represents a fit to the data. The measured shift in the minimum of the modulation pattern, from about –60° in Figure 10 to about –10° in Figure 11 is consistent with the change in polarization angle of the incident beam (to within the accuracy of the experimental setup).

Further testing is currently underway to more completely characterize the performance of the science model. This will include a more complete analysis of several runs made at a variety of different energies, along with a more complete comparison with simulations of the laboratory setup.

5. HARD X-RAY POLARIMETRY OF SOLAR FLARES

The principle motivation for studying the polarization of hard X-rays from solar flares is that such data can provide important information regarding the the extent to which the accelerated electrons are beamed during the flaring process. This would have potentially important implications for any model of solar flare particle acceleration. Only with polarization measurements can we probe the extent of the electron beaming for individual flares. Previous attempts to measure X-ray polarization from solar flares have been limited to energies below ~30 keV and the available data generally provides conflicting results on the X-ray polarization of solar flares. SOLPOL is designed to operate at higher energies (above 50 keV), where the contaminating effects of thermal X-ray emission can be minimized.[11] (The contamination in this case results from the polarization of initially unpolarized photons as a result of backscattering from the photosphere.) Theoretical models predict a range of possible polarization levels for the hard X-ray emission. In general, polarization levels as high as 10-15% can be expected.[12]

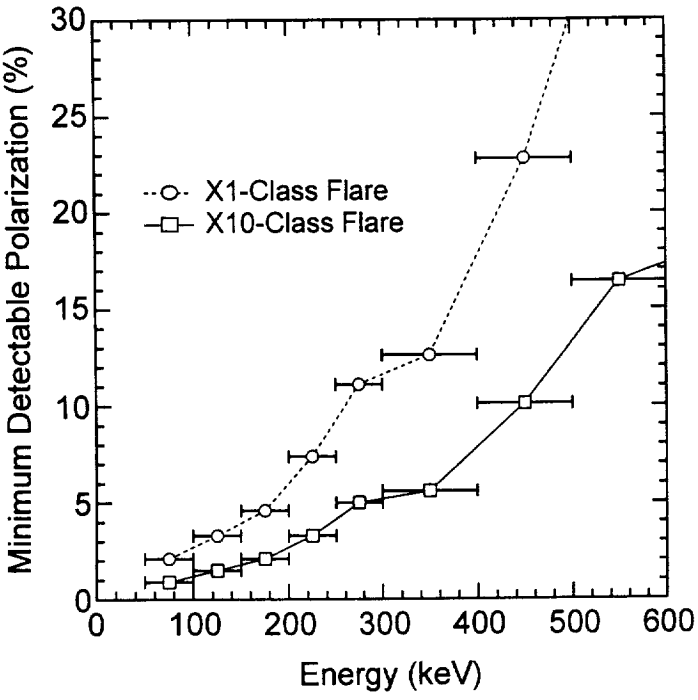

Figure 12: Estimates for the minimum detectable polarization (MDP) of a 16-element balloon-borne SOLPOL array in various energy bands for two different size solar flares.

In practice, the SOLPOL design would be used in the context of an array of polarimeter modules. Such an array could be made an integral part of either a long-duration balloon payload or an Earth-orbiting spacecraft payload. It is difficult to make specific predictions about the sensitivity of such an array to any one flare due to the unique nature of each individual flare event. We have, however, estimated the polarization sensitivity based on the SMM-measured spectrum for the flare of 7 June 1980. The assumed background is that of a balloon-borne payload. The resulting sensitivity estimates indicate that an array of sixteen modules would provide a minimum detectable polarization (MDP) of less than 1% in the integrated 50-300 keV energy range for some M-class flares and all X-class flares. Alternatively an array of four modules would provide a MDP of 1% or better in the integrated 50-300 keV energy range for all X-class flares. Figure 12 shows the MDP that is attained in smaller energy bands using a 16-element SOLPOL array for an X1- and an X10-class flare. MDP levels of a few percent should be sufficient to test various models for hard X-ray polarization in solar flares.

Another potential application for a SOLPOL-type module would be as a polarimeter that could be placed on the Particle Acceleration Solar Orbiter (PASO). PASO is a program currently being considered as a next-generation high energy solar observatory (part of the future roadmap for NASA's Sun-Earth Connection program). With a launch date of ~2012 (during solar maximum), it would be placed into a solar orbit at ~0.2 AU for observing high energy emissions from solar flares. At that distance, a single SOLPOL module would have the sensitivity equivalent to that of a 25-element SOLPOL array at 1 AU.

6. SUMMARY

The goal of the science model testing is to verify the performance characteristics of the SOLPOL design and to define the final electronics configuration. Once this has been accomplished, we can move forward with the detailed design and fabrication of a self-contained engineering model. We anticipate that this design would be used in the context of an array of polarimeter modules. An array of 16 modules would be capable of measuring solar flare polarization levels below 1% for the X-class flares and would also be capable of measuring polarization levels down to about 15% in some of the largest γ-ray bursts.[5] Although similar designs have been discussed in the literature,[11,13] we are unaware of any other active effort to develop specilaized hardware for measuring polarization in solar flares or in γ-ray bursts at energies above 100 keV.

In addition to its potential for studying transient sources, the SOLPOL design might also be useful in the context of an imaging polarimeter. For example, a SOLPOL element or array of elements could be used with a rotation modulation collimator to achieve arc-second angular resolution. Such an approach is not unlike that employed for hard X-ray imaging (without polarization capability) in the upcoming HESSI mission.[14] The spatial information intrinsic to the SOLPOL design might also be useful in a coded-aperture system, although perhaps limited to arc-minute angular resolutions.

ACKOWLEDGEMENT

This work has been supported by NASA grants NAGW-5704 and NAG5-7294.

REFERENCES

1. R.D. Evans, The Atomic Nucleus, New York: McGraw-Hill, 1958.
2. R. Novick, "Stellar and solar X-ray polarimetry," *Space Science Reviews*, vol. 18, pp. 389-408, 1975.
3. F. Lei, A.J. Dean and G.L. Hills, "Compton scatter polarimetry in gamma-ray astronomy," *Space Science Reviews*, vol. 82, pp. 309-388, 1997.
4. M. McConnell, D. Forrest, K. Levenson, and W.T. Vestrand, "The design of a gamma-ray burst polarimeter," in AIP Conf. Proc. 280, *Compton Gamma-Ray Observatory*, M. Friedlander, N. Gehrels and D.J. Macomb, Eds. New York: AIP, 1993, pp. 1142-1146.
5. M.L. McConnell, D.J. Forrest, J. Macri, J.M. Ryan, and W.T. Vestrand, "Development of a hard X-ray polarimeter for gamma-ray bursts," AIP Conf. Proc. 428, *Gamma-Ray Bursts*, C.A. Meegan and P. Cushman, Eds. New York: AIP, 1998, pp. 889-893.
6. M.L. McConnell, D.J. Forrest, J. Macri, M. McClish, M. Osgood, J.M. Ryan, W.T. Vestrand and C. Zanes "Development of a hard X-ray polarimeter for solar flares and gamma-ray bursts," *IEEE Trans. Nucl. Sci.*, vol. 45, no. 3, pp. 910-914, June, 1998.
7. H. Sakurai, M. Noma, and H. Niizeki, "A hard x-ray polarimeter utilizing Compton scattering," in *SPIE Conf. Proc.*, vol. 1343, pp.512-518, 1990.
8. W.H. McMaster, "Matrix representation of polarization," *Reviews of Mod. Phys.*, vol. 33, no. 1, pp. 8-28, January 1961.
9. M.L. McConnell, J.R. Macri, M. McClish, J. Ryan, D.J. Forrest and W.T. Vestrand, "Development of a Hrad X-Ray Polarimeter for Astrophysics," *IEEE Trans. Nucl. Sci,* in press, 1999.
10. R. Wojcik, S. Majewski, B. Kross, D. Steinbach, and A.G., "High spatial resolution gamma imaging detector based on a 5" diameter R3292 Hamamatsu PSPMT," *IEEE Trans. Nucl. Sci.*, vol. 45, no. 3, pp. 487-491, June, 1998.
11. G. Chanan, A.G. Emslie, and R. Novick, "Prospects for solar flare X-ray polarimetry," *Solar Physics*, vol. 118, pp. 309-319, 1988.
12. F. Lei, A.J. Dean, and G.L. Hills, "Compton polarimetry in gamma-ray astronomy," *Sp. Sci. Rev.*, vol. 82, pp. 309-388, 1997.
13. T.L. Cline, et al., "A gamma-ray burst polarimeter study," in *Proceedings of the 25th Internat. Cosmic Ray Conf.*, vol. 5, pp. 25-28, 1997.
14. .R. Dennis, et al., "The High Energy Solar Spectroscopic Imager – HESSI," in *SPIE Conf. Proc.*, vol. 2804, pp.228-240, 1996.

26th ICRC (Salt Lake City) (1999)

SH.1.2.07

A Polarimeter for Studying Hard X-Rays from Solar Flares

M.L. McConnell, J.R. Macri, M. McClish, J.M. Ryan

[1] *Space Science Center, University of New Hampshire, Durham, NH 03824, USA*

Abstract

We present a modular design for a Compton scatter polarimeter that will be used for studying the polarization of hard X-rays (50-300 keV) from solar flares. A complete polarimeter module fits on the front end of a 5-inch position-sensitive photomultiplier tube (PSPMT). The PSPMT is used to determine the Compton interaction location within an annular array of small plastic scintillator elements. Some of the photons that scatter within the plastic scintillator are subsequently absorbed by a small centrally-located array of CsI crystals that is read out by an independent multi-anode PMT. The independence of the two PMT readout schemes provides appropriate timing information. Monte Carlo simulations indicate that one such module, with a scintillator thickness of 12.7 cm, has a peak effective area of almost 3.5 cm^2 at 200 keV and a polarization modulation factor in excess of 50% from 50 keV up to 250 keV. A small array of such detectors would be capable of measuring polarization levels of less than 1% in X-class solar flares. We are currently testing a fully-functional science model based on this design concept. These tests are designed to evaluate the performance characteristics of the design and to more fully validate our Monte Carlo simulation code. Here we shall review the characteristics of this modular design and report on the status of the laboratory testing. We will also outline the potential of this design for performing polarization measurements of solar flares, including the possibility of incorporating such detectors into an imaging polarimeter.

1 Introduction:

The basic physical process used to measure linear polarization of hard X-rays (50–300 keV) is Compton scattering. The successful design of a polarimeter at these energies hinges on the ability to reconstruct the kinematics of each Compton scatter event. In this context, we can consider: 1) the ability to measure the energies of both the scattered photon and the scattered electron; and 2) the ability to measure the scattering geometry.

A Compton scatter polarimeter consists of two detectors that are used to measure the energies of both the scattered photon and the scattered electron (e.g., Novick 1975; Lei, Dean & Hills 1997). These measurements also serve to define the scattering geometry. One detector (the *scattering detector*) provides the medium for the Compton interaction to take place. This detector must be designed to maximize the probability of a single Compton interaction with a subsequent escape of the scattered photon. The second detector (the *calorimeter*) absorbs the remaining energy of the scattered

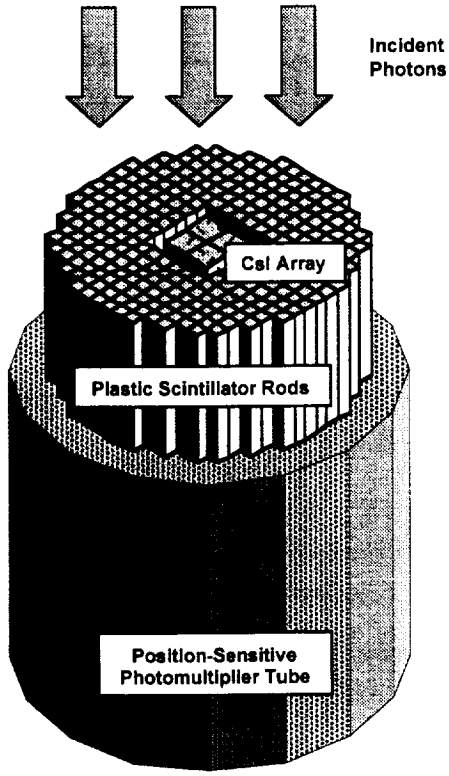

Figure 1: The modular design showing the layout of the plastic scintillator elements and CsI elements on the front surface of a PSPMT. As shown here, the depth of the detector elements is 5.08 cm. Not shown is the MAPMT used to readout the CsI elements.

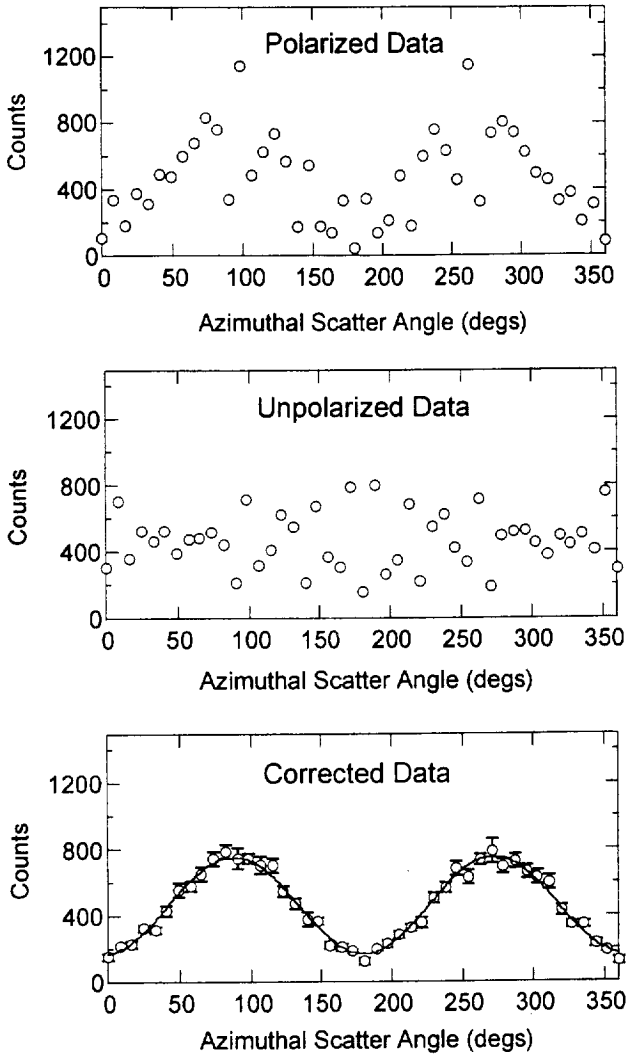

Figure 2: Simulated polarimeter data showing how the measured data is corrected for intrinsic geometric effects to extract the true modulation pattern. These data correspond to the response of the baseline SOLPOL design to a monoenergetic beam of polarized 150 keV photons incident at 0°.

photon. The accuracy with which the scattering geometry can be measured determines the ability to define the modulation pattern and has a direct impact on the polarization sensitivity.

The spatial resolution can easily be improved by using arrays of smaller detector elements, where the element size determines the spatial resolution. Using a large number of detection elements typically requires a correspondingly large number of electrical channels.

2 A Modular Polarimeter Design:

We have developed a modular polarimeter design that places an entire device on the front end of a single 5-inch diameter PSPMT, as shown in Figure 1 (McConnell et al., 1998a, 1999). This approach provides high spatial resolution, but significantly reduces the number of readout channels. This design, which we call SOLPOL (for SOLar POLarimeter) incorporates an array of 5 mm × 5 mm optically-isolated plastic scintillator elements arranged in the form of an annulus having an outside diameter of 10 cm (corresponding to the sensitive area of the Hammatsu R3292 5-inch PSPMT). The central portion of the annulus is large enough to insert a 2 × 2 array of optically-isolated 1 cm CsI scintillators. The CsI array is coupled to an independent 4-anode MAPMT (Hamamatsu R5900-04) for energy measurement and signal timing.

An ideal event is one in which the incident photon Compton scatters in one plastic element, with the remaining photon energy subsequently absorbed in the central CsI array. The small cross-sectional area of each scintillator element ensures that practically all multiple scatter events are rejected.

A series of Monte Carlo simulations have been used to determine the charcteristics of the SOLPOL design. The energy threshold levels, particularly in the scattering elements, have a significant influence on the performance of the polarimeter at low energies. These simulations assume threshold energies of 15 keV in the plastic and 50 keV in the CsI. Figure 2 illustrates the nature of the simulated data. The first panel shows the polarization response to a fully polarized monoenergetic beam of 150 keV photons vertically incident on the front surface of the polarimeter. This distribution includes not only the intrinsic modulation pattern due to the Compton scattering process, but also the geometric effects related to the specific layout of

the detector elements within the polarimeter and the associated quantization of possible scatter angles. The geometric effects can be more clearly seen in the case of an incident beam that is completely unpolarized, as shown in the second panel of Figure 2. To extract the true distribution of polarized events, we divide the polarized distribution by the unpolarized distribution (as determined either by simulations or direct measurement) and normalize by the average of the unpolarized distribution, yielding the expected cos 2θ modulation pattern (the third panel of Figure 2).

Figures 3 and 4 show the characteristics of the SOLPOL design, in terms of the effective area and modulation factor, respectively, as a function of incident photon energy. In both cases, we show the results for two different detector depths. The deeper detector presents an advantage in terms of effective area, while having little influence on the modulation factor. In practice, the advantage of increased effective area for the deeper detector must be offset by the decrease in light collection efficiency and the increase in detector background.

One potentially useful aspect of the SOLPOL design is that there exists a significant polarization response at large off-axis angles. This can be seen in Figure 5, which is based on simulations with a detector depth of 5.08 cm. The effective area remains relatively constant at large angles, a result of the fact that the exposed geometric area of the detector remains relatively constant. Although there is a decrease in the modulation factor at large angles, there is still significant polarization response even at 60° incidence angle. The off-axis response of this design would be especially useful, for example, in studies of γ-ray bursts.

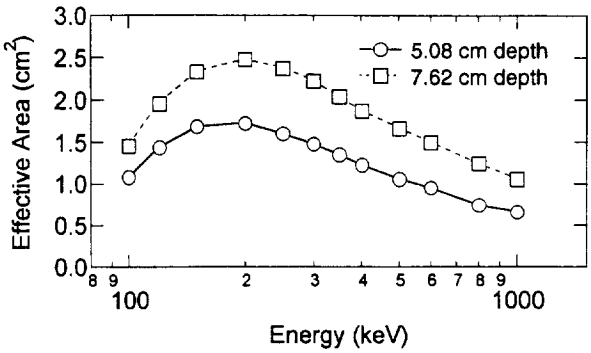

Figure 3: The effective area as a function of energy.

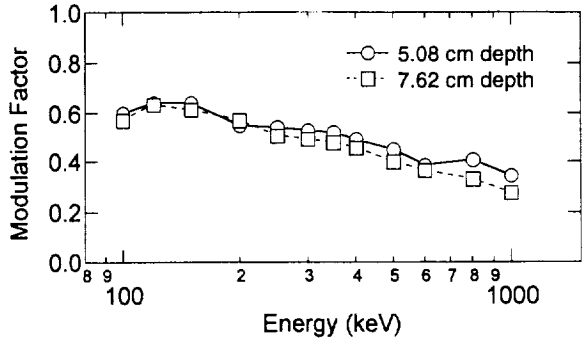

Figure 4: The modulation factor as a function of energy.

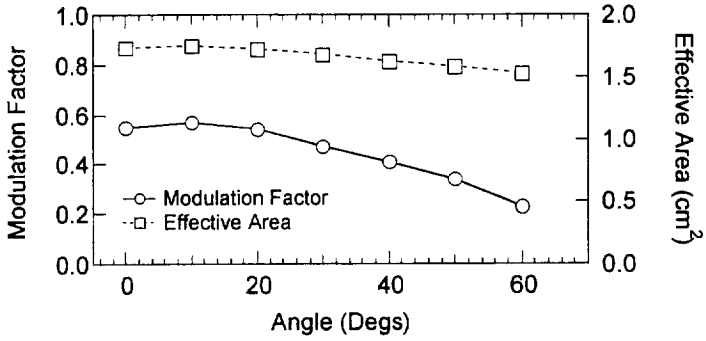

Figure 5: The modulation factor and effective area at 200 keV for various incidence angles. The polarimeter maintains good response out to 60° incidence angles.

3 Recent Laboratory Testing:

We have very recently completed the fabrication of a science model based on the modular SOLPOL design. The initial tests make use of a charge division network for the PSPMT (Hammamatsu R3292) that provides a weighted average of the spatial distribution of the measured light output using only four anode signals. In the future, we will gain more precise information regarding the distribution of energy deposits

within the plastic by using the 56 (28-x plus 28-y) anode signals from the PSPMT. Given the mean free path of photons in plastic (6 cm at 100 keV), we expect that a high level of multiple scatter event rejection can be achieved using a readout scheme that relies on only a fraction of the 56 anode signals, thus minimizing the required number of electrical channels.

Figure 6 shows the spatial distribution of events within the plastic array. Photons from a ^{137}Cs source were used to uniformly illuminate the front surface of the polarimeter. Only those events that were coincident in both the plastic and the CsI are registered. The individual 5 mm plastic elements are clearly resolved by the PSPMT. These data suggest that even smaller elements could be used with this PSPMT. We are still in the process of completing the setup and energy calibration of this science model, after which we will proceed with tests using polarized photons

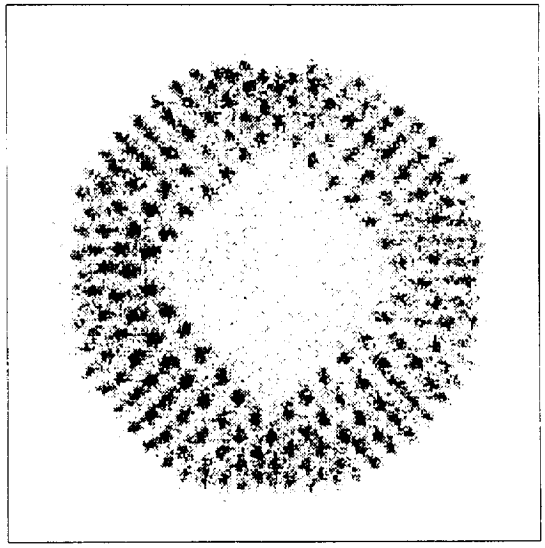

Figure 6: Distribution of measured polarimeter events within the plastic array. These are events (from ^{137}Cs) which scatter between the plastic elements and the central calorimeter. The spatial resolution of the PSPMT clearly distinguishes individual 5mm plastic elements.

4 Solar Flare Polarimetry:

The measurement of hard X-ray polarization in solar flares would be useful in studying the directivity of flare-accelerated electrons (e.g., Chanan, Emslie & Novick 1988). We anticipate that this design may be used in the context of an array of polarimeter modules. An array of 4 modules, for example, would be capable of measuring sensitivity levels in the 50-300 keV range of less than 1% in X-class flares. A larger array of 16 modules would also be capable of measuring polarization levels down to ~5% in some of the largest γ-ray bursts (McConnell et al. 1998b).

The SOLPOL design might also be useful in the context of an imaging polarimeter. For example, a SOLPOL element or array of elements could be used with a rotation modulation collimator to achieve arc-second angular resolution. Such an approach is the same as that employed for hard X-ray imaging in the upcoming HESSI mission. Imaging polarimetry with arc-second spatial resolution would open up the possibility of measuring polarization at various locations within the flare region, providing detailed information about the geometry of the accelerated electron beam.

References

Chanan, G., Emslie, A.G., and Novick, R. 1988 *Solar Physics*, 118, 309.

Lei, F., Dean, A.J., and Hills, G.L. 1997, Sp. Sci. Rev., 82, 309.

McConnell, M.L. et al. 1998a, IEEE Trans. Nucl. Sci., 45(3), 910.

McConnell, M.L. et al. 1998b, AIP Conf. Proc. 428, *Gamma-Ray Bursts*, C.A. Meegan and P. Cushman, Eds. New York: AIP, 889.

McConnell, M.L. et al. 1999, to be published IEEE Trans. Nucl. Sci.

Novick, R. 1975, Sp. Sci. Rev., 18, 389.